Hindawi
Advances in Civil Engineering
Volume 2018, Article ID 1594546, 11 pages
https://doi.org/10.1155/2018/1594546

Research Article

Formation Mechanism and Mechanical Properties of Soil-Rock Mixture Containing Macropore

Feng Zhu, Wei Qian, Huilin Le, Haotian Fan, and Wuchao Wang

School of Earth Science and Engineering, Hohai University, Nanjing 211100, China

Correspondence should be addressed to Feng Zhu; 578971556@qq.com

Received 15 June 2018; Revised 20 October 2018; Accepted 8 November 2018; Published 11 December 2018

Academic Editor: Annan Zhou

In southwestern China, soil-rock mixture containing macropore (SRMCM) is very common in large-scale accumulation slopes. The formation mechanism and mechanical parameters of SRMCM play an important role in slope stability. In this paper, we designed a new physical model test to study the formation mechanism of SRMCM. We analyzed different factors that influence the formation of SRMCM. The mechanical properties of SRMCM are obtained by direct shear test. New physical model test demonstrates the best slurry consistency (30%) and slope angle (35°~45°) to form SRMCM. The results of direct shear test show that the strength parameters of SRMCM are high and it is influenced by the angle of macropore structure. When the angle of macropore structure increases, so does the cohesion of SRMCM. In this process, the internal friction angle does not change much.

1. Introduction

SRMCM (soil-rock mixture containing macropore) is a special type of soil-rock mixture, in which, macropore structure is defined as an accumulation of gravels without clay formed in different stratum of slopes. Figure 1 shows that SRMCM always appears with local stratification in deep-thick accumulation slopes, which is different from common soil-rock mixture (Figure 2). The formation mechanism and mechanical parameters of SRMCM play an important role in slope stability. However, the study of SRMCM has not been conducted.

In southwestern China, SRMCM is very common in large-scale accumulation slopes. The slope angles vary from 35° to 45°, and there are a lot debris flow deposits. The annual precipitation is 600 mm~800 mm, and the rainfall is usually heavy. The slope angles, debris flow, and rainfall might be the cause for SRMCM. To date, no experiments have ever been conducted to determine the best slurry consistency and slope angle to form SRMCM.

Inside SRMCM, binder bonds the particles in point state. The binder is upper soil that can move down to coarse particle layer by leaching. From field investigation, many slopes in southwestern China have very steep ditch banks on both sides of the gully. The free face is almost vertical after rainfall erosion on slope edge for many years. The steep slope of SRMCM can stay stable rather than collapse and sliding during an earthquake. It is important to study the mechanical properties of SRMCM during the evaluation of talus slide.

An inhomogeneous rock-soil system consists of high-strength stone, fine-particle soil, and pores. The strength characteristics of this system depend on rock and soil thresholds, visual grain size, and stone [1]. An unconventional in situ shear test apparatus is used to investigate the strength properties of the shale-limestone chaotic complex (SLCC) bimrock [2, 3]. A generalized conceptual empirical approach is used to predict the overall strength of unwelded bimrocks and bimsoils [4]. There is little field investigation of SRMCM. No field shear test and empirical method have ever been proposed for the mechanical properties of SRMCM.

In laboratory, CT scan and fluctuation method are used to reconstruct the 3D model of gravel to study content, feature size, and soil-gravel distribution [5, 6]. Indoor shear test is used to obtain mechanical characteristics of unsaturated soil-rock mixture [7–10]. Afifipour and Moarefvand [11, 12] used a servo-control machine to conduct

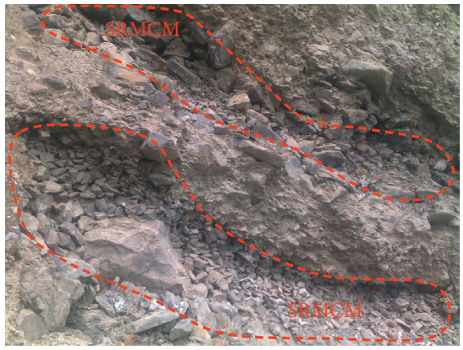

Figure 1: Soil-rock mixture containing macropore (SRMCM).

Figure 2: Soil-rock mixture (SRM).

uniaxial compression tests on model bimrocks to obtain mechanical parameters such as uniaxial compressive strength (UCS), Young's modulus, failure strain, and full-scale stress-strain curves. Ergenzinger et al. [13], Xu et al. [14–16], and Zhao et al. [17] used discrete element method (DEM) to investigate the strength and failure properties of SRMS in shear zone. Particle flow code (PFC) 3D is developed to establish a stochastic structural model and simulate pressure shear deformation damage test [9]. Ding et al. [18] and Meng et al. [19] established a numerical simulation method based on microstructures. This method is reasonable after comparison with indoor test results.

In this paper, we develop a physical model test to study the formation mechanism of SRMCM. This simulates the formation process of SRMCM, and different factors in this process are considered. Mechanical properties of SRMCM are analyzed by indoor tests. Our parameters can be used as a reference in slope stability evaluation of Mahe talus slide at Lenggu hydropower station.

2. Formation Mechanism of Macropore Structure

2.1. Field Investigation of SRMCM in Mahe Talus Slide. Mahe talus slide is located in downstream of Mahe opposite to the concealed bend of Caiyu highway. The natural slope of Mahe talus slide is gentle rubble and the width on upper surface is narrower than lower surface. The angle of the slope varies from 30° to 35°. Ephemeral gully development occurs inside.

The gravels in SRMCM come from the crushed rock layer. The bedrock surface of Mahe talus slide is antidip, and it is made of heavily crushed metamorphic sandstones. Joint fissure develops fully. Figure 3 shows the existing collapse conditions. The distribution of SRMCM layers is random, and the collapsing gravels cave along the slope from the top to accumulate in concave slope surface.

Figure 3(a) shows that there are many cementing soil-rock mixtures overlying or underlying the SRMCM. Due to the short distance between cementing soil-rock mixtures and the ground surface, the soil-rock mixtures are not cemented by gravity; rather, they are cemented as slurry-stone fragmental materials flowing along the slope and accumulating on the crushed rock layer. The fragmental materials are generated at the top part of slope on rainstorm conditions. The thickness of slurries on the crushed rock layer ranges from 50 to 100 cm. This thin layer of slurries is formed because of the relatively high velocity. Figure 3(b) shows the transitional zone of slurry-stone fragmental materials flowing on crushed rock layer. Only the leaching of mussy water can be seen on the surface of crushed rock layer. Figure 3(b) shows the multilayer SRMCM in Mahe talus slide. In dry climate, the SRMCM may be formed by endless superposition of cementation layers. These layers emerge after quick dehydration and consolidation of slurry. The drilling in the middle of Mahe talus slide reveals that SRMCM may exist on the bedrock-cover discontinuity and been buried deeply. Figure 4 shows the boundary of Mahe talus slide.

2.2. Size Distribution Test. On the complex terrain of Mahe talus slide, we collected ten groups of samples from five slide parts for size distribution test. Figure 5 shows the samples being collected from Mahe talus slide.

Figure 6 shows the grading analysis curve of ten samples. Table 1 gives particle composition of the ten samples.

To remove the super-size particles for the indoor tests, the scalping method was chosen for the grain size > 60 mm. The soil can still be in natural gradation after the scalping. However, the nonuniform coefficient C_u would change, and thus, the integral strength of soil. The content of gravel after scalping is calculated in formula (1):

$$p_i = \frac{p_{0i}}{(100 - p_{d\max})}, \quad (1)$$

where p_i denotes the content of gravel after scalping, p_{0i} denotes the content of gravel before scalping, and $p_{d\max}$ denotes the content of super-size gravel.

Table 2 shows the particle composition of soil after scalping.

2.3. Formation Test of the Macropore

2.3.1. Properties of the Test Material. Soil, gravels, and water are used as materials to prepare the slurry. The soil and gravels are taken from Mahe talus slide. Figure 7(a) shows the prepared soil with particle diameter < 5 mm. Figure 7(b) shows the gravel with different diameters, 5 mm~10 mm,

(a) (b)

Figure 3: Formation mechanism of the SRMCM. (a) SRM overlying or underlying the SRMCM. (b) The multilayer SRMCM in Mahe talus slide.

10 mm~20 mm, and 20 mm~30 mm. The three groups of gravels are mixed to the mass ratio of 1 : 2 : 1.

2.3.2. The Model Test Tank Which Can Alter Angle. The model test tank (Figure 8) was made of four parts as follows:

(1) *Floor*. The materials for the floor are transparent acrylic sheets with size of 120 cm × 60 cm. Grooves are set on the floor to fix the foreplate and backboard, and to change the width of SRMCM. The intervals of groove are 30 cm, 40 cm, and 50 cm.

(2) *Foreplate and Backboard*. The foreplate and backboard of the size 120 cm × 80 cm are made of transparent organic glass with thickness of 2 cm. Four circular holes of diameters 10 mm are set in the base angles of glass to intercalate the bolts to fix the foreplate and backboard. 8 circular holes of diameters 10 mm are set in the middle of glass with radiation distribution to intercalate the bolts to fix the middle part of the steel plate. The four angles between the 8 circular holes above and the horizontal are 15°, 25°, 35°, and 45°, respectively. Intercalating the bolts into different holes would change the angles of baffle.

(3) *Multiangle Baffle*. The baffle is made of stainless steel plate of thickness 5 mm. From the statistics of relief intensity of mountain landslide, three undulation angles are set in the middle of the baffle to simulate the mountain undulation angles. Three different widths of 30 cm, 40 cm, and 50 cm are set for every angle. Twelve stainless steel plates are made to simulate the formation process of SRMCM.

(4) *Bolts*. The bolts are stainless steel of the diameter 8 mm. Two herringbone nuts are put in every bolt for dismounting.

2.3.3. Test Procedure. Sixteen independent tests are made. We performed every test twice to reduce errors.

(1) Preparation of SRM slurry. After the soil samples of 60 kg weight and the gravel samples of 18 kg (30% weight of the soil samples) were mixed averagely, the water of 15.6 kg was put in to prepare the SRM slurry of 26% consistence. The SRM slurry prepared above was then stirred uniformly and placed for 30 minutes after being covered with plastic film. Figure 9 shows the SRM slurry after being stirred uniformly.

(2) The floor was put in a relatively wide field; two organic glasses with 16 fixing holes were set in the necks whose interval is 30 cm. 8 fixing holes were set in each glass, and the bolts were intercalated in these holes. The nuts were in neither too tight nor too loose to make sure the steel plate could be put in successfully. Type I steel plate was put inside the organic glasses with the inclination angle of which to be 15°, and the bolts were calated to fix the steel plate.

(3) The mixed gravels were paved on the steel plate with the thickness of 5 cm. After that, the SRM slurry was poured onto the steel plate. Then, the process of slurry invading into macropore space was recorded by taking photos. According to the thickness of macropore space, whether the macropore structure can form in a different angle or not was known. At last, the thickness of macropore structure was recorded.

(4) The formed SRMCM would be sunned for 15~20 d to air-dry in a drying and ventilating area.

(5) The angle set in step (2) was changed to 25°, 35°, and 45°, and then step (3) and step (4) were repeated. Steps (2), (3), and (4) were repeated with the consistence of SRM slurry changing to 30%, 32%, and 34%. The relationship of slope angle, thickness of macropore structure, and the angle was observed under different consistence.

(6) In step (5), four SRMCM samples with the size of 15 cm × 15 cm × 15 cm were taken out in each angle and were baked in oven for 24 hours under the 110°C constant temperature. Then all 32 samples were tested by shear test. Figure 10 shows the test procedure of macropore structure formation.

2.3.4. Test Results

(1) Relationship between Slope Angle, Slurry Consistency, and Macropore Structure Formation. Four slurries were prepared with different water contents of 26%, 30%, 32%, and 34%. The model test tank was set with four different angles of 15°,

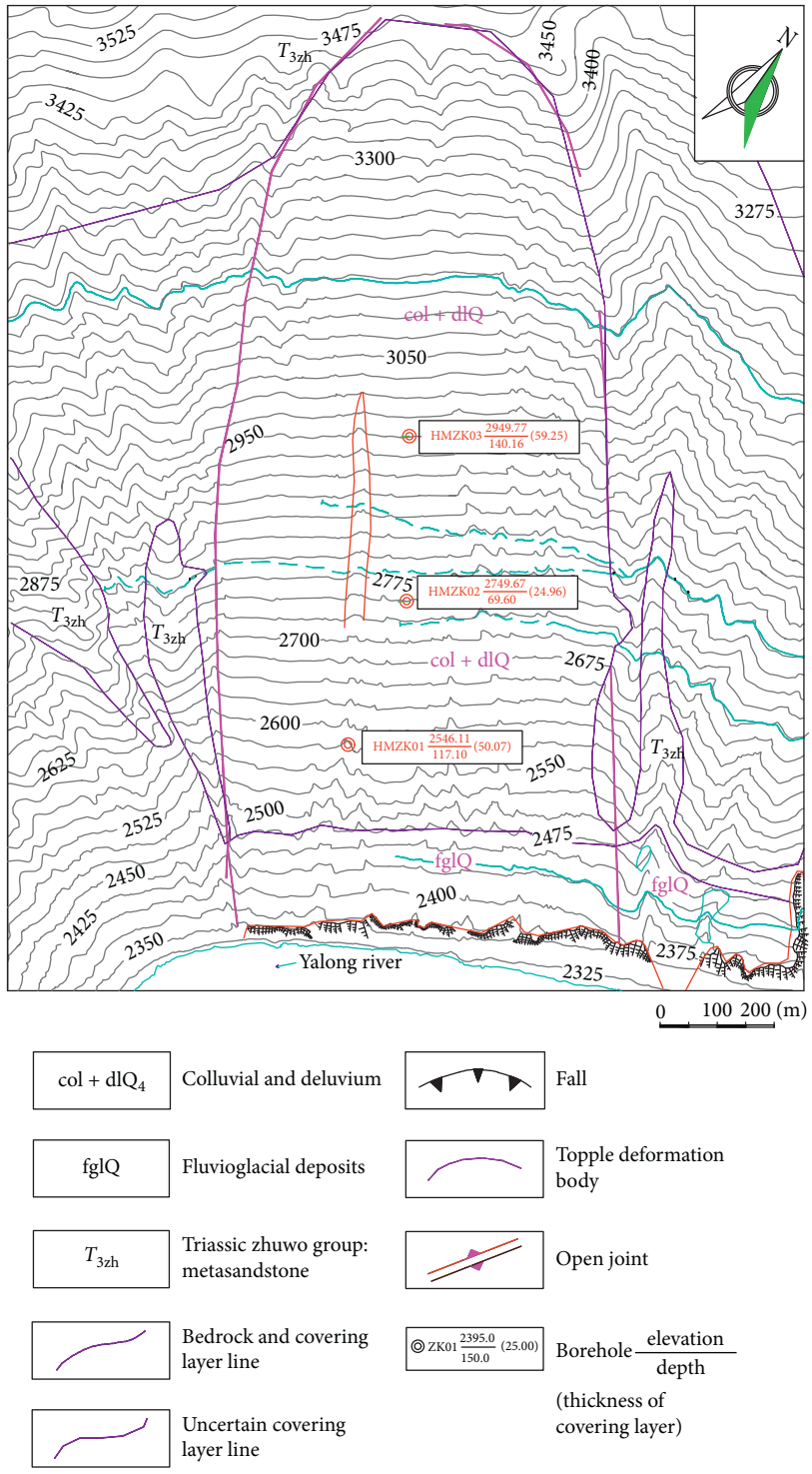

Figure 4: Boundary of Mahe talus slide.

25°, 35°, and 45° according to the field statistics of undulation angle of slope. After doing 16 unrepeated tests in which the model test tank with different angles and the slurries with different consistence were combined, and Table 3 shows the relationship between slope angle, slurry consistence, and macropore structure formation.

According to Table 3, in the 16 tests, the macropore structure formed in 8 tests while not formed in the other 8 tests. The test results show that macropore structure forms in a certain slope when the SRM slurries of certain consistence invade into crushed rock layer. In gentle slope, macropore structure cannot form as the fluidity of the slurries with dense consistence is low, which makes the component force of down flow small and the slurries can hardly flow down. With the increase of water content in slurries, the consistency of slurries becomes more and more diluted and macropore structure forms as the slurries flow down slowly along the face of slope with the decreasing of downward

Figure 5: Samples being collected from Mahe talus slide.

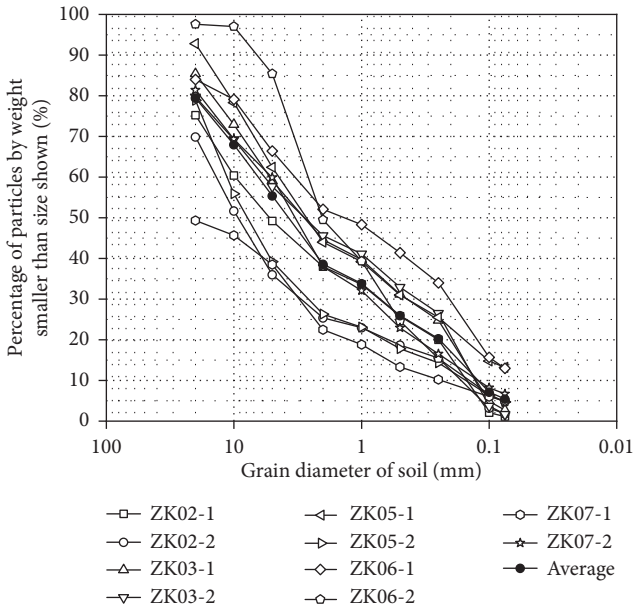

Figure 6: Grading analysis curve of ten samples.

Table 1: Particle composition of the ten samples.

Name of the particle	Range of particle size (mm)	Content of gravels (%)	Average content (%)
Gravel	>60	4.05~11.0	7.34
	>5	47.25~74.20	61.22
	0.075~5	20.31~29.48	23.49
Silt	0.005~0.075	3.7~8.6	5.59
Clay	<0.005	6.0~13.9	9.7

Table 2: Particle composition of samples after scalping.

Name of the particle	Range of particle size (mm)	Content of gravels (%)	Average content (%)
Gravel	>5	50.3~72.5	60.1
	0.075~5	20.52~29.72	23.8
Soil particles	0.005~0.075	4.3~10.5	6.4
	<0.005	6.0~16.3	9.7%

resistance. With the increasing of slope angle, the component force of down flow becomes bigger and bigger despite the low water content and dense consistence. After that, the slurries invade the crushed rock layer, the rear slurries push the frontage slurries to flow down continuously, and the macropore structure forms. When the angle of slope increases to a certain degree and the slurries dilute enough, the slurries flow down along the face of slope quickly with a thin layer of slurries on the crushed rock layer. Meanwhile, only little part of slurries invade the crushed rock layer, while more slurries flow down along the face of slope under gravity action, thus makes the macropore structure forming hardly.

(2) Relationship between Slope Angle, Slurry Consistency, and Thickness of Macropore Structure. The thicknesses of macropore structure must be different as the consistencies of slurries and thicknesses of slurries invading the crushed rock layer are different. In the tests, the designed thickness of crushed rock layer is 5 cm. Figure 11 shows the thicknesses of macropore structure layers under different slope angles in the tests.

According to Figure 11, under same water contents of mud, the density (thickness) of macropore increases when the dip angle of macrospore structure becomes larger (from 15° to 45°), because the larger dip angle makes downward resistance decrease, and the increasing fluidity makes the thickness of invading smaller. The thickness of macropore ranges from 15 mm to 40 mm. When the dip angle increases to a certain degree, most slurries flow down along the face of slope and there is no thickness of macropore structure, as the macropore structure cannot form. Under same slope angle, with the increase of the water contents of slurry, the consistency becomes smaller, the fluidity of SRM slurry increases, and the thickness of invading slurries become bigger firstly, then become smaller. Under the interaction of changing the consistence and slope angle, the density (thickness) of macropore structure changes little in one range of slope angle with the changing consistency. That is, macropore structure forms most easily with the slope angle of 35°, which is basically the same with the slope angle of Mahe talus slide (as is shown in Figure 4). It is hard to form the macropore structure when the slope is too gentle or too steep.

3. Shear Strength Parameter Tests of the SRMCM

20 samples of SRMCM were taken to carry out indoor direct shear test, and they were divided into four groups. In every

(a) (b)

Figure 7: Soil and Gravel samples. (a) Soil sample. (b) Gravel samples.

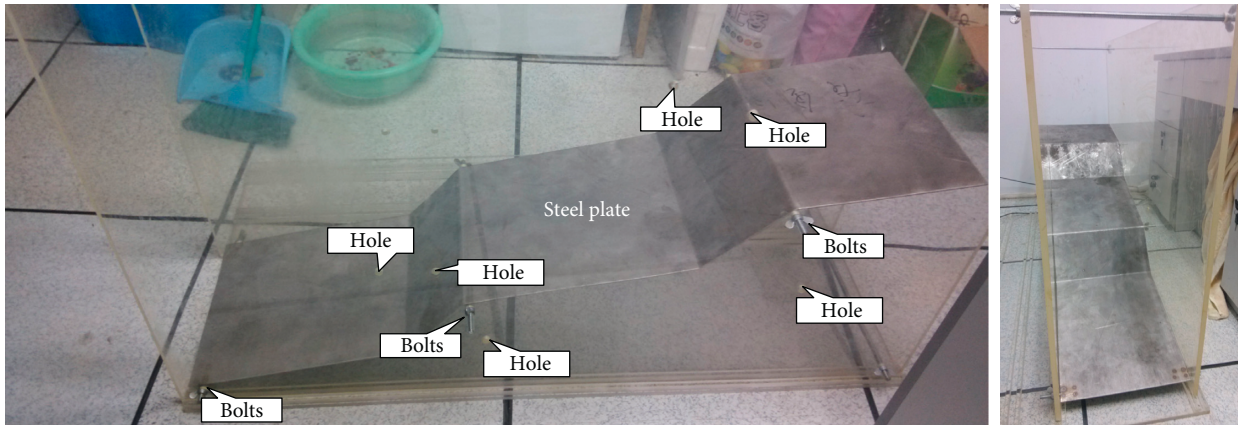

Figure 8: Model test tank which can alter the angle.

Figure 9: SRM slurry.

group, the size of samples was 15 cm × 15 cm × 15 cm. The samples with different angles of macropore structure in SRMCM as 15°, 25°, 35°, and 45° were prepared based on the model test tank. The samples whose angle of macropore structure in SRMCM is 0° were prepared as the control group. All the samples were put in dry and ventilated conditions for 15–20 d to completely air-dry. Figure 12 shows the samples of SRMCM before indoor direct shear test.

3.1. Test Procedure. The tests were carried out under normal pressures of 100, 200, 300, and 400 kPa to define the shear strength parameters. In the test, the loading rate in every step was controlled in same level and not over 0.2 mm/min. Pressure sustained for a period after shear failure, and the residual strength was determinate. The loading stopped if shear displacement kept increasing or was more than 15 mm. Normal stress would be relieved before shear stress

(a) (b)

Figure 10: Test procedure of macropore structure formation. (a) The process of making the sample. (b) Final sample.

Table 3: Relationship between slope angle, slurry consistence, and macropore structure.

Undulation angles (°)	Content of water (%)			
	26	30	32	34
15°	×	×	×	√
25°	×	×	×	√
35°	×	√	√	√
45°	√	√	√	×

"√" means the macropore structure can form; "×" means the macropore structure cannot form.

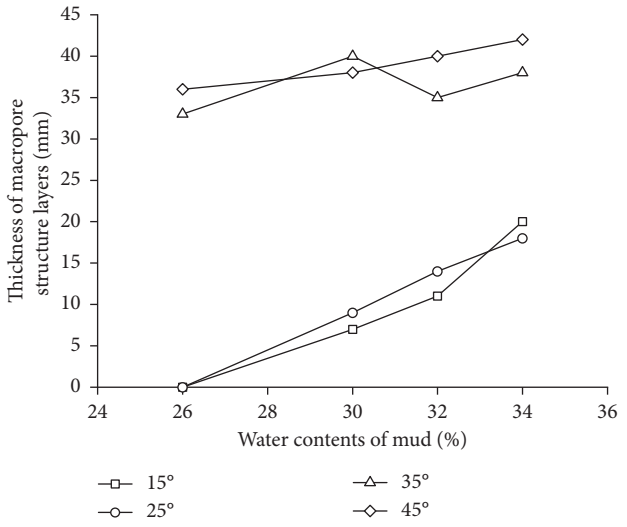

Figure 11: Thickness of macropore structure layers.

in pressure relief. Figure 13 shows the samples of SRMCM after indoor direct shear test.

3.2. Test Results. According to the results of indoor direct shear test, Figure 14 shows the curves of shear stress and shear displacement in different angles of macropore structure.

The results of indoor direct shear test are listed as follows:

Figure 12: Samples of SRMCM before the indoor direct shear test.

Figure 13: Samples of SRMCM after the indoor direct shear test.

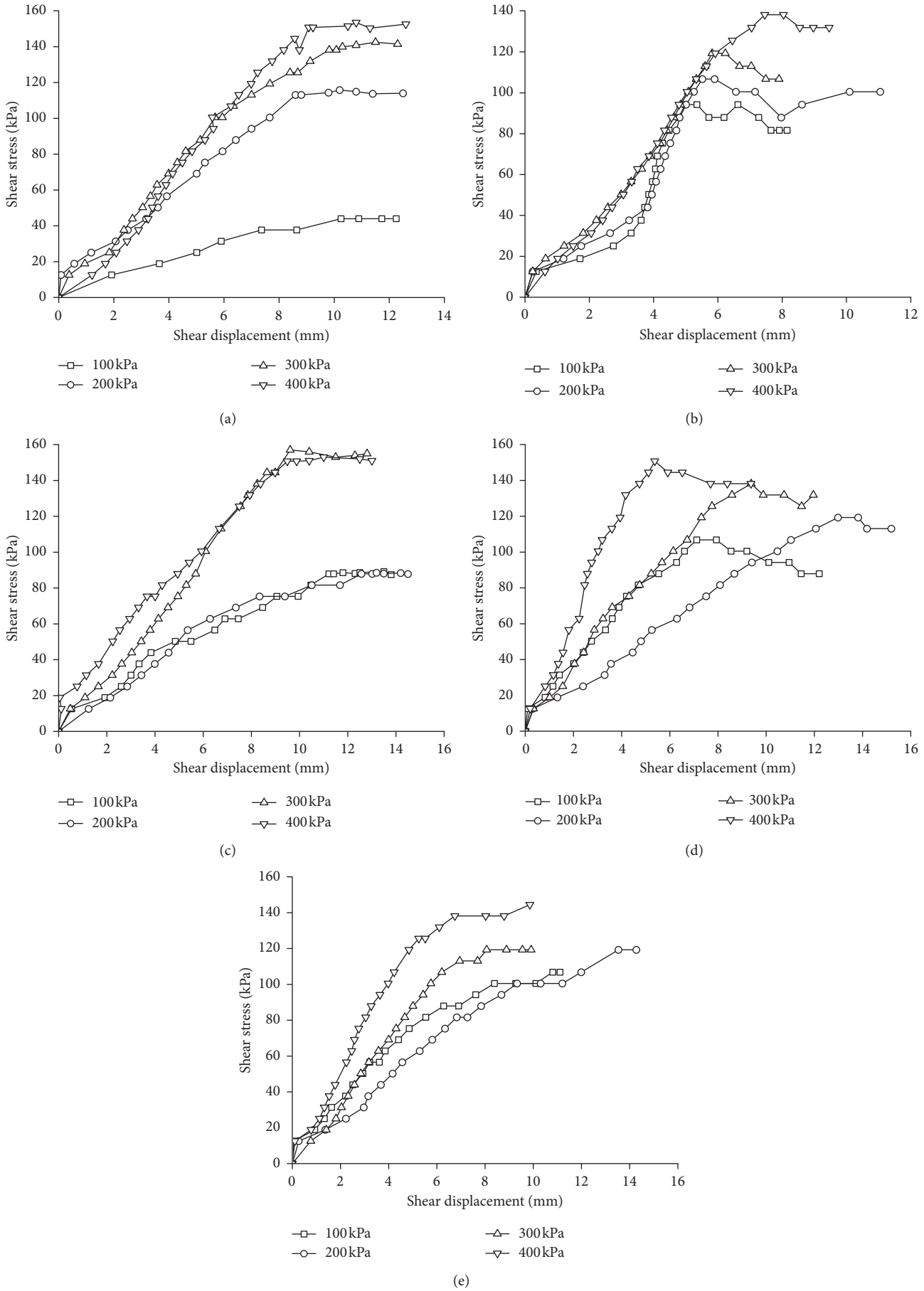

Figure 14: Curves of shear stress and shear displacement in different angles of macropore structure. (a) 0°, (b) 15°, (c) 25°, (d) 35°, and (e) 45°.

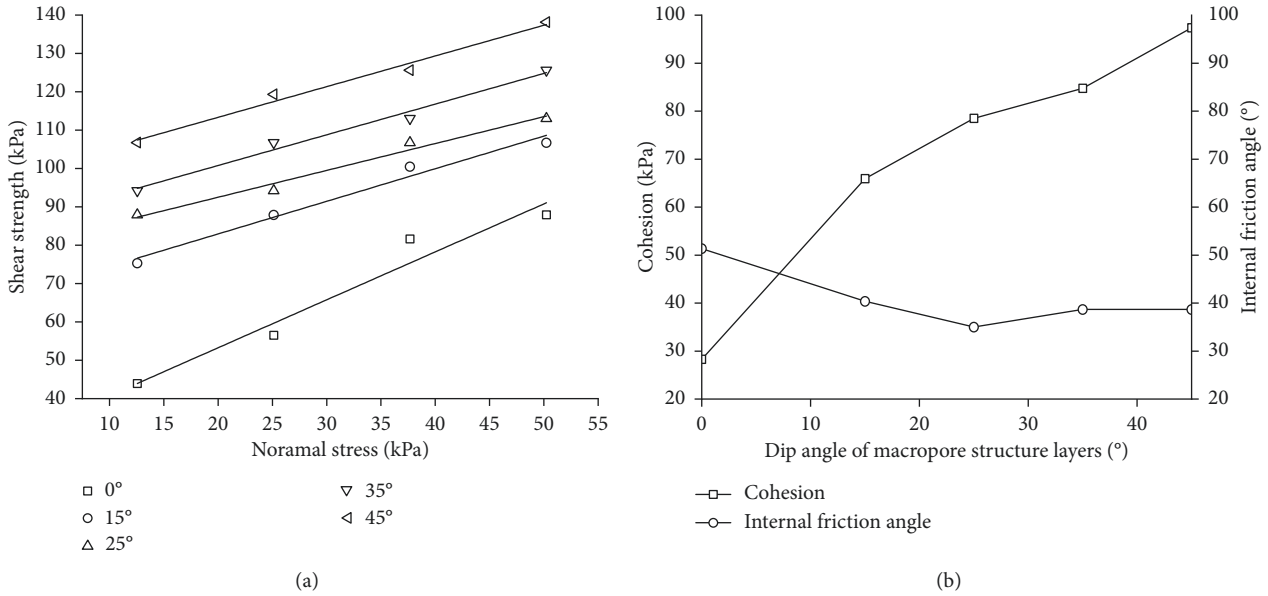

Figure 15: Shear strength of SRMCM in different angles of macropore structure. (a) Fitting curves of different angle. (b) Relationship between strength parameters and different dip angles.

(1) With the increase of axial compression, the strength of SRMCM increases gradually, and the strength changes obviously in different axial compression. When the angle of macropore structure in SRMCM is 0°, the change of SRMCM strength is especially obvious in different axial compression. That is because the macropore structure is happened to be on and parallel to the shear surface. The shear strength of SRMCM is decided by the bite force between the gravels in macropore structure and has no relationship with the bond strength between fine soil. So, when in low axial compression, the gravels can throw over the gravels nearby with small bite force and low strength.

(2) When the angle of macropore structure in SRMCM increases, the hardening degree of SRM sample increase gradually. When in same shear displacement, the larger the macropore structure angle is, the higher the strength is, especially in angle of 45°. In angle of 45°, the shear strength is beyond 130 kPa when the displacement is 4 mm. With the increase of macropore structure angle, the angle between shear zone and macropore structure becomes larger. Two SRM layers encapsulate the macropore structure, with the increase of shear strength, the inclined macropore structure will surely stagger unconnected, the gravels on shear zone will roll mutually, and one part of the gravels will inlay the SRM nearby. Under a certain axial compression, the inlaying will cost quite large energy with the external expression of shear strength increasing.

(3) Figure 14 shows that the macropore structure is one stable structure, and the strength of macropore structure does not have apparent peak no matter either in a big or small angle. After reaching a high level, the shear stress sustains a high state but not gets the apparent tendency of decreasing. The shear stress will not increase while the shear displacement keeps increasing when the horizontal load is applied continually, rather than the common material failure whose shear stress decreases apparently after failure.

(4) According to the curves of shear stress and shear displacement, the shear strengths in different axial compression are obtained. Figure 15 shows the stress curve gotten by fitting the shear strengths in different axial compression with the using of Mohr–Coulomb theory.

According to Figure 15, the cohesion of macropore structure is very large except when the angle of macropore structure is 0°, and with the increase of angle, cohesion keeps enlarging while internal friction angle changes little. When the dip angle of macrospores is low, the cohesion depends on the sliding friction of the fine-grained soil. When dip angle of macrospores is high, the number of macrospores is large and the cohesion depends on the sliding friction of fine-grained soil, the friction of soil and rock, and the contact force of rocks. When dip angle of macrospores keeps increasing, the number of macrospores keeps increasing, the contact force of rocks keeps increasing, and the cohesion keeps increasing. When the angle of macropore structure is 0°, the cohesion is very small while the internal friction angle is very large because of the interaction of gravels but not of soil particles. When under shearing, the angles of macropore structure are different from that of the shear plane, the upper and lower shear planes stagger unconnected, and macropore structure staggers unconnected. Due to the bite force between the gravels, the gravels must bypass the gravels nearby to produce the displacement that enlarges the shear strength.

4. Conclusion

In this paper, Mahe talus slide of the Lenggu hydropower station was used as an example. Field investigation was used to know the structural properties of SRMCM in Mahe talus slide. The formation mechanism of SRMCM was analyzed by a new physical model test. The mechanical properties of SRMCM were analyzed by indoor direct shear test. The main conclusions of the study include the following:

(1) The SRMCM is one stable structure forming in a certain slope when the SRM slurries of certain consistence invade into the crushed rock layer.

(2) The formation of SRMCM is closely related to the consistence of slurries. The SRMCM cannot form with the consistency too high or too low. The test shows that in water content of 30%, the slurries flow most fluently, and the SRMCM forms most easily. In the physical model test, the thickness of macropore structure forming with 35°~45° slope angle is the largest; that is, the SRMCM forms most easily with 35°~45° slope angle in real.

(3) The shear strength of SRMCM is very high. When the angle of macropore structure keeps increasing, the cohesion keeps enlarging while internal friction angle changes little. It deepens the understanding of the slope failure mechanism when there are SRMCMs in the slope.

Data Availability

The data used to support the findings of this study are available from the corresponding author upon request.

Conflicts of Interest

The authors declare that there are no conflicts of interest regarding the publication of this paper.

Acknowledgments

This research was financially supported by the Natural Science Foundation of China (grant no. 41672258) and Postgraduate Research and Practice Innovation Program of Jiangsu Province (no. KYCX17_0501). This research was also supported by "The Fundamental Research Funds for the Central Universities" (no. 26120172017B665X1). The authors gratefully acknowledge M.S. Penglei XU in School of Earth Sciences and Engineering, Hohai University, China, for his contribution to the laboratorial experiment.

References

[1] W. Xu and R. Hu, "Conception, classification and significations of soil-rock mixture," *Hydrogeology and Engineering Geology*, vol. 36, no. 4, pp. 50–56, 2009.

[2] N. Coli, P. Berry, and D. Boldini, "In-situ non-conventional shear tests for the mechanical characterisation of a bimrock," *International Journal of Rock Mechanics and Mining Sciences*, vol. 48, no. 1, pp. 95–102, 2011.

[3] Z. L. Zhang, W. J. Xu, W. Xia, and H. Y. Zhang, "Large-scale in-situ test for mechanical characterization of soil-rock mixture used in an embankment dam," *International Journal of Rock Mechanics and Mining Sciences*, vol. 86, pp. 317–322, 2016.

[4] H. Kalender, E. Sonmez, C. Medley, K. Tunusluoglu, and E. Kasapoglu, "An approach to predicting the overall strengths of unwelded bimrocks and bimsoils," *Engineering Geology*, vol. 183, pp. 65–79, 2014.

[5] S. Li, D. Zhang, S. S. Du, and B. Shi, "Computed tomography based numerical simulation for triaxial test of soil-rock mixture," *Computers and Geotechincs*, vol. 73, pp. 179–188, 2016.

[6] H. Y. Zhang, W. J. Xu, and Y. Z. Yu, "Triaxial tests of soil-rock mixtures with different rock block distributions," *Soils and Foundations*, vol. 56, no. 1, pp. 44–56, 2016.

[7] S. Sun, P. Xu, J. Wu et al., "Strength parameter identification and application of soil–rock mixture for steep-walled talus slopes in southwestern China," *Bulletin of Engineering Geology and the Environment*, vol. 73, no. 4, pp. 123–140, 2014.

[8] H. Z. Wei, W. J. Xu, X. F. Xu, Q. S. Meng, and C. F. Wei, "Mechanical properties of strongly weathered rock-soil mixtures with different rock block contents," *International Journal of Geomechanics*, vol. 18, no. 5, article 04018026, 2018.

[9] D. F. Cen, D. Huang, and F. Ren, "Shear deformation and strength of the interphase between the soil-rock mixture and the benched bedrock slope surface," *Acta Geotechnica*, vol. 12, no. 2, pp. 391–413, 2017.

[10] B. Zhao, W. Huang, Z. Shu, M. Han, and Y. Feng, "Experimental and theoretical studies on the creep behavior of bayer red mud," *Advances in Civil Engineering*, vol. 2018, Article ID 6327971, 9 pages, 2018.

[11] M. Afifipour and P. Moarefvand, "Mechanical behavior of bimrocks having high rock block proportion," *International Journal of Rock Mechanics and Mining Sciences*, vol. 65, no. 1, pp. 40–48, 2014.

[12] M. Afifipour and P. Moarefvand, "Experimental study of post-peak behavior of bimrocks with high rock block proportions," *Journal of Central South University*, vol. 21, no. 2, pp. 761–767, 2014.

[13] C. Ergenzinger, R. Seifried, and P. Eberhard, "A discrete element model predicting the strength of ballast stones," *Computers and Structures*, vol. 108-109, no. 4, pp. 3–13, 2012.

[14] W. J. Xu, S. Wang, H. Y. Zhang, and Z. L. Zhang, "Discrete element modelling of a soil-rock mixture used in an embankment dam," *International Journal of Rock Mechanics and Mining Sciences*, vol. 86, pp. 141–156, 2016.

[15] W. J. Xu, L. M. Hu, and W. Gao, "Random generation of the meso-structure of a soil-rock mixture and its application in the study of the mechanical behavior in a landslide dam," *International Journal of Rock Mechanics and Mining Sciences*, vol. 86, pp. 166–178, 2016.

[16] W. J. Xu, C. Q. Li, and H. Y. Zhang, "DEM analyses of the mechanical behavior of soil and soil-rock mixture via the 3D direct shear test," *Geomechanics and Engineering*, vol. 9, no. 6, pp. 815–827, 2015.

[17] Q. Zhao, N. Zhang, R. Peng, G. Li, C. Han, and Y. Guo, "Discrete element simulation of roadway stability in an efflorescent oxidation zone," *Advances in Civil Engineering*, vol. 2018, Article ID 4183748, 15 pages, 2018.

[18] X. Ding, H. Zhang, S. Huang, B. Lu, and Q. Zhang, "Research on mechanical characteristics of unsaturated soil-rock mixture based on numerical tests of mesostructured," *Chinese*

Journal of Rock Mechanics and Engineering, vol. 31, no. 8, pp. 1554–1566, 2012.

[19] Q. X. Meng, H. L. Wang, W. Y. Xu, and M. Cai, "A numerical homogenization study of the elastic property of a soil-rock mixture using random mesostructure generation," *Computers and Geotechnics*, vol. 98, pp. 48–57, 2018.